# Temperature Dependence of Structural and Mechanical Properties of Isotactic Polypropylene

**Daniel J. Lacks[†] and Gregory C. Rutledge***

*Department of Chemical Engineering, Massachusetts Institute of Technology, Cambridge, Massachusetts 02139*

*Received August 22, 1994; Revised Manuscript Received October 27, 1994[⊗]*

ABSTRACT: Finite-temperature simulations of crystalline isotactic polypropylene are carried out self-consistently using a molecular mechanics force field for the interatomic potential and quasi-harmonic lattice dynamics for the vibrational free energy. Negative axial thermal expansion is observed, in agreement with experiment, and is attributed to elastic coupling to the transverse thermal stresses. The axial elastic modulus decreases with temperature, due to entropic effects and as a consequence of transverse thermal expansion, which acts to increase the unstrained volume and move the system to a region of the potential energy surface with lower curvature. The transverse and off-diagonal elastic moduli decrease with temperature, due to a decrease in the curvature of the potential energy surface as the chains move apart with thermal expansion.

## I. Introduction

The properties of polymer crystals are somewhat unusual due to their extreme anisotropy. Although there has been much success in explaining general aspects of the structural and elastic properties of polymer crystals in terms of the molecular architecture,[1] a similar clarification of the temperature dependence of these properties has been lacking. Many studies of "generic" polymer properties have been based on the simplest polymer, polyethylene (PE), which is characterized by a planar zigzag conformation. Isotactic polypropylene (iPP) represents an important test for this line of reasoning; the chemical constitution of iPP is the same as that of PE, but the pendant methyl side groups of iPP induce the formation of a $3_1$ helical conformation of the polymer chain rather than the planar zigzag conformation of PE. We have carried out simulations of the temperature dependence of the properties of polymer crystals, treating thermal expansion and elasticity from first principles, without any *ad hoc* assumptions. The results for polyethylene (PE)[2] and the aromatic polyamides poly(*p*-phenylene terephthalamide) (PPTA) and poly(*p*-benzamide) (PBA)[3] have been previously reported, as well as some thermal expansion results for iPP.[4] The present paper describes elasticity results and more extensive thermal expansion results for iPP.

Thermal expansion and elasticity are related properties, as the elastic moduli depend on the equilibrium structure determined by thermal expansion, and the extent of thermal expansion depends on the elastic response of the material to thermally-induced stresses. The isothermal stiffness moduli, $C^{\mathrm{T}}{}_{ij}$ (using Voigt notation), can be defined by[5]

$$C^{\mathrm{T}}{}_{ij} = \frac{1}{V_T}\left[\frac{\partial^2 A}{\partial\epsilon_i \partial\epsilon_j}\right]_{T,\epsilon_{k\neq i,j}} \tag{1a}$$

$$C^{\mathrm{T}}{}_{ij} = \frac{1}{V_T}\left[\frac{\partial^2 U_{\mathrm{pot}}}{\partial\epsilon_i \partial\epsilon_j}\right]_{T,\epsilon_{k\neq i,j}} + \frac{1}{V_T}\left[\frac{\partial^2 U_{\mathrm{vib}}}{\partial\epsilon_i \partial\epsilon_j}\right]_{T,\epsilon_{k\neq i,j}} - \frac{T}{V_T}\left[\frac{\partial^2 S}{\partial\epsilon_i \partial\epsilon_j}\right]_{T,\epsilon_{k\neq i,j}} \tag{1b}$$

where $A$ is the Helmholtz free energy, $U_{\mathrm{pot}}$ is the potential energy, $U_{\mathrm{vib}}$ is the vibrational energy, $S$ is the entropy, $T$ is the temperature, $V_T$ is the unstrained volume at temperature $T$, and $\epsilon_j$ is the $j$ component of the strain. The temperature dependence of the $C^{\mathrm{T}}{}_{ij}$ arises explicitly from the entropic term and the temperature dependence on the quantum mechanical vibrational energy and entropy, and also as a consequence of thermal expansion, which changes both the unstrained volume $V_T$ and the local shape of the potential energy surface (by changing the reference state at which the second derivatives are taken).[6]

Thermal expansion as the elastic response to thermal stresses may be recognized in the following equality:[5]

$$\alpha_i = \frac{C_{\mathrm{v}}}{V}\sum_{j=1}^{6}\gamma_j S^{\mathrm{T}}{}_{ij} \tag{2}$$

where $C_{\mathrm{v}}$ is the heat capacity at constant volume and $S^{\mathrm{T}}{}_{ij}$ is the isothermal compliance modulus (related to the stiffness modulus by $\mathbf{S} = \mathbf{C}^{-1}$). The thermal stress, $(C_{\mathrm{v}}/V)\gamma_j$, is determined by the change in entropy with strain,[5]

$$\gamma_i = \frac{1}{C_{\mathrm{v}}}\frac{\partial S}{\partial\epsilon_i} \tag{3}$$

where $\gamma_i$ is the Gruneisen parameter. Thus thermal expansion along one axis is the resultant elastic response to the thermal stresses along *all* axes.

## II. Computational Method

The free energy of the crystal is calculated within the quasi-harmonic approximation, with the interatomic potential parameterized by a molecular mechanics force field. The equilibrium unit cell volumes are obtained from first principles by minimizing the free energy at the specified temperature. Elastic constants and Gruneisen parameters are obtained from the appropriate

[†] Present address: Department of Chemical Engineering, Tulane University, New Orleans, LA 70118.

[⊗] Abstract published in *Advance ACS Abstracts,* January 1, 1995.

0024-9297/95/2228-1115$09.00/0 

**Table 1. Nonbonded Parameters Used in the Present Simulations (See Equations 4 and 5)**

| | KDG[a] | SLKB* |
|---|---|---|
| $A_{CC}$ (kJ/mol) | 125 629 | 125 520 |
| $A_{HH}$ (kJ/mol) | 7063 | 7113 |
| $B_{CC}$ (1/Å) | 3.38 | 3.40 |
| $B_{HH}$ (1/Å) | 3.54 | 3.61 |
| $C_{CC}$ (kJ/mol) | 1975 | 1883 |
| $C_{HH}$ (kJ/mol) | 180 | 172 |

[a] These parameters are the same in the KDG* force field.

numerical derivatives of the free energy and entropy with strain. Detailed descriptions of our computational method have already been reported.[2,4] These calculations are for perfectly crystalline systems and therefore do not include effects due to the noncrystalline fractions which may be important in real polymer materials.

**a. Free Energy Calculation.** The vibrational free energy is evaluated within the quasi-harmonic approximation,[7] in which terms higher than second order in the Taylor expansion of the potential energy are neglected. The resulting harmonic potential energy surface and vibrational frequencies vary with the lattice parameters, thereby incorporating anharmonic effects due to volume changes but neglecting the anharmonic coupling of the vibrational modes. Also, the expansion of the potential energy about a local minimum precludes effects which may occur at higher temperatures if the system visits different potential energy minima. Quantum mechanical effects, which are important for vibrational motion with frequencies $\nu > kT/h$ ($\approx$200 cm$^{-1}$ at room temperature), are included. An analysis of the accuracy of the quasi-harmonic approximation and perturbative corrections is given elsewhere.[8]

The equilibrium lattice parameters are those which minimize free energy, which is the sum of the potential energy and the vibrational free energy. The free energy for a given set of lattice parameters is obtained by first minimizing the potential energy with respect to the variables describing the atomic positions within the unit cell and then calculating the vibrational frequencies for points in the Brillouin zone and integrating numerically the free energy for these vibrational frequencies over the Brillouin zone.

**b. Force Fields.** The calculations were carried out with modifications of the molecular mechanics force fields of Sorensen *et al.*[9] (SLKB) and Karasawa *et al.*[10] (KDG), which we designate SLKB* and KDG*. The KDG* force field differs from the KDG force field in that force constants were included for the CCC–CCC and CCC–CCH bend–bend interactions. As the KDG force constants for the other bend–bend interactions range from 19 to 32 kJ/mol, we arbitrarily chose the force constants for the CCC–CCC and CCC–CCH interactions to be equal to 25.0 kJ/mol, the center of this range. We tested the effect of these new force constants by comparing the calculated vibrational frequencies of isobutane with experimental results and found that the accuracy of the vibrational frequencies for isobutane is similar to that for polyethylene, for which the KDG force field was designed.

The SLKB* force field differs from the original SLKB force field in the form and the parameters of the nonbonded interaction terms. The form for the nonbonded interactions in the SLKB* force field is the same as that in the KDG force field, less any Coulombic interactions,

$$E_{ab}(r) = A_{ab}e^{-B_{ab}r} - C_{ab}/r^6 \tag{4}$$

where

$$A_{ab} = (A_{aa}A_{bb})^{1/2}$$

$$B_{ab} = \frac{1}{2}(B_{aa} + B_{bb})$$

$$C_{ab} = (C_{aa}C_{bb})^{1/2} \tag{5}$$

and the values for the parameters are given in Table 1. This functional form has the advantage over the original SLKB functional form in that geometric mean mixing rules are used for the dispersion constants, making the computational time for the reciprocal space Ewald sum proportional to the number of atoms in the unit cell, rather than the *square* of the number of atoms in the unit cell.[11] This greatly reduces the computational time for iPP, where $N = 108$ and the reciprocal space sum must be carried over many unit cells because of the large unit cell size. The SLKB* nonbonded parameters were obtained by fitting to experimental results for polyethylene: In particular, we fit the exp-6 parameters to reproduce the low-temperature PE lattice parameters and cohesive energy, using the quantum zero temperature approach (i.e., minimized potential energy plus zero-point vibrational energy).

**c. Crystal Structure.** The minimum-energy configuration for the iPP chain is a $3_1$ helix, which is formed when the backbone torsion angles alternate between trans and gauche (Figure 1a). The most stable crystalline phase of iPP, as suggested by both experiment[12] and calculation,[13,14] is the $\alpha_2$ phase. The $\alpha_2$ structure is based on a monoclinic unit cell with four chains, and three monomer units per chain, in the unit cell (see Figure 1b).[15] Chains 1 and 2 are mirror images of each other and have their methyl groups pointing upward, and chains 3 and 4 are mirror images of each other and have their methyl groups pointing downward.[16]

We consider the four iPP chains within the unit cell to be equivalent, as is found experimentally. The variables describing the atomic positions in the unit cell are the Cartesian coordinates of the atoms in the first chain (except for four coordinates which are fixed—the setting angle is varied instead of one of these coordinates, and the other three coordinates are fixed to define the unit cell), the setting angle for the first chain, and the setting angle and three translational offset coordinates for all other chains. Therefore, a total of 90 degrees of freedom are used to describe the positions of the atoms within the unit cell. In addition, the six parameters defining the unit cell are varied during free energy minimization.

## III. Results

The equilibrium lattice parameters as a function of temperature for iPP are shown, and compared with the experimental room temperature results,[17] in Figure 2. The shift between the KDG* and the SLKB* results is due, at least in part, to the differences in the nonbonded parametrizations (i.e., fitting classical or quantum calculations to experimental results). The thermal expansion coefficients are given in Table 2 and are compared to experimental results.[18–20] Negative axial thermal expansion is found at all temperatures. The agreement between simulation and experiment is good for $\alpha_1$ and $\alpha_3$, but the calculated $\alpha_2$ is significantly less

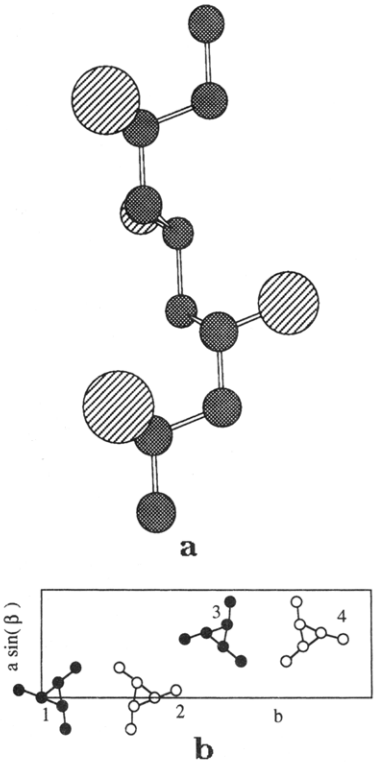


**Figure 1.** (a) Chain configuration of iPP. The darker atoms represent backbone carbon atoms, and the lighter atoms represent methyl carbons; hydrogen atoms are omitted for clarity. (b) $\alpha_2$ structure of iPP, projected onto the $[a \sin \beta]-b$ plane.

than is found experimentally and does not reflect the experimentally observed anisotropy.

The complete set of elastic moduli are given in Table 3. The precision of these values is approximately ±1 GPa, due to the error arising from numerical evaluation of the second derivative in eq 1; this imprecision limits the analysis of elastic moduli with small temperature dependences. The elastic stiffness matrices calculated with the SLKB* and KDG* force fields are similar and are in substantial agreement with the earlier static–lattice calculation of Tashiro *et al.*[21] The present $C_{33}$ (at 300 K) is larger than that of Tashiro *et al.* by 12–22 GPa, and the present $C_{13}$ is larger by 3 GPa; all other stiffness constants are within 2 GPa of those of Tashiro *et al.*

The axial Young's modulus (defined as $1/S_{33}$) at room temperature is calculated to be 49 GPa for the SLKB* force field and 58 GPa for the KDG* force field. These results are consistent with the result of 41 GPa from X-ray diffraction experiments[22] and the result of 36 GPa from mechanical experiments on ultradrawn iPP,[23] as these techniques generally underestimate the true crystalline modulus in polymer materials.[24] The present axial Young's moduli are close to the value of 37 GPa estimated from Raman scattering experiments[25] and the value of 40 GPa calculated by Tashiro *et al.*[21]

The Gruneisen parameters for iPP are shown in Figure 3. All of the Gruneisen parameters are positive, indicating that increases in entropy accompany expansions along all axes.

## IV. Discussion

**a. Thermal Expansion.** *1. Axial Thermal Expansion.* Axial thermal expansion is the sum of the elastic responses to the thermal stresses along *all* coordinates, as shown in eq 2. Since the axial Gruneisen parameter of iPP is positive, contraction along the chain axis leads to an unfavorable decrease in entropy. The observed axial thermal contraction must be due to the elastic response to the lateral thermal stresses.[4] The contributions to the axial thermal expansion from thermal effects both along and transverse to the chain axis are given in Table 4 and support this explanation of axial thermal contraction in iPP. This mechanism differs from previously proposed mechanisms of axial thermal contraction in polymer materials, which are based on entropy increases associated with axial contraction.[26–31] Our studies on other polymer materials concluded that both mechanisms of negative axial thermal contraction are operative in PE, PPTA, and PBA. In PE, the entropy increase associated with contraction is the dominant effect, as shown in Table 4. In PPTA and PBA, as for iPP, elastic coupling to transverse thermal stresses is the dominant effect, even though these polymers were found to have negative axial Gruneisen parameters.[3]

*2. Transverse Thermal Expansion.* The present calculations, with both the SLKB* and KDG* force fields, find the transverse thermal expansion coefficients $\alpha_1$ and $\alpha_2$ to be similar in magnitude. The calculated $\alpha_1$ is in good agreement with experiment, but the calculated $\alpha_2$ is significantly lower than observed experimentally.[18] This underestimation of the $\alpha_2$ is related to an underestimation of the linear compressibility, $\beta$ ($\beta_i = \sum_{j=1}^{3} S^{T}_{ij}$), along the $b$ axis as compared to the experimental data of Ito[32] (shown in Figure 4) and was observed in earlier static–lattice calculations of Tashiro *et al.*[21] These authors suggest that the disagreement between calculation and experiment for the linear compressibilities is due to entropic effects arising from the methyl group torsional vibration. They corrected for this effect by using mode Gruneisen parameters for this vibrational mode obtained from fitting calculated linear compressibilities to experimental data. Although good agreement with experiment could then be obtained for the linear compressibilities, very poor agreement with experiment was obtained for the thermal expansion coefficients, resulting in $\alpha_1$ of the wrong sign. While there are good arguements for questioning the sufficiency of a quasi-harmonic approximation to represent the methyl torsional motion in iPP, it would appear that these *ad hoc* corrections may overcompensate. The current method derives all Gruneisen parameters self-consistently and admits, via perturbation theory, an extension to test for the importance of local anharmonicity in one or more modes.

Another possible cause of the disagreement may be that the experimentally determined ratio $\alpha_1/\alpha_2$ is sensitive to finite lamellar size. The data of Davis *et al.* for polyethylene, for example, exhibits almost a factor of 2 variation between samples with lamella thicknesses of 99 and 385 Å.[30] Experiments on iPP have shown that the $b$ lattice parameter varies with the thermal history of the samples, those samples annealed near the melting point having smaller $b$ dimensions[13] and presumably lower $\alpha_2$ and $\beta_2$ as a result. The calculations, of course, assume infinite crystallite size.

**b. Temperature Dependence of Elastic Moduli.** *1. Axial Stiffness Modulus.* Temperature dependences of $C^{T}_{ij}$ arise not only from the vibrational free energy but also as a consequence of thermal expansion, which affects $C^{T}_{ij}$ through changes in the unstrained volume $V$ and the value of the second derivative of the potential

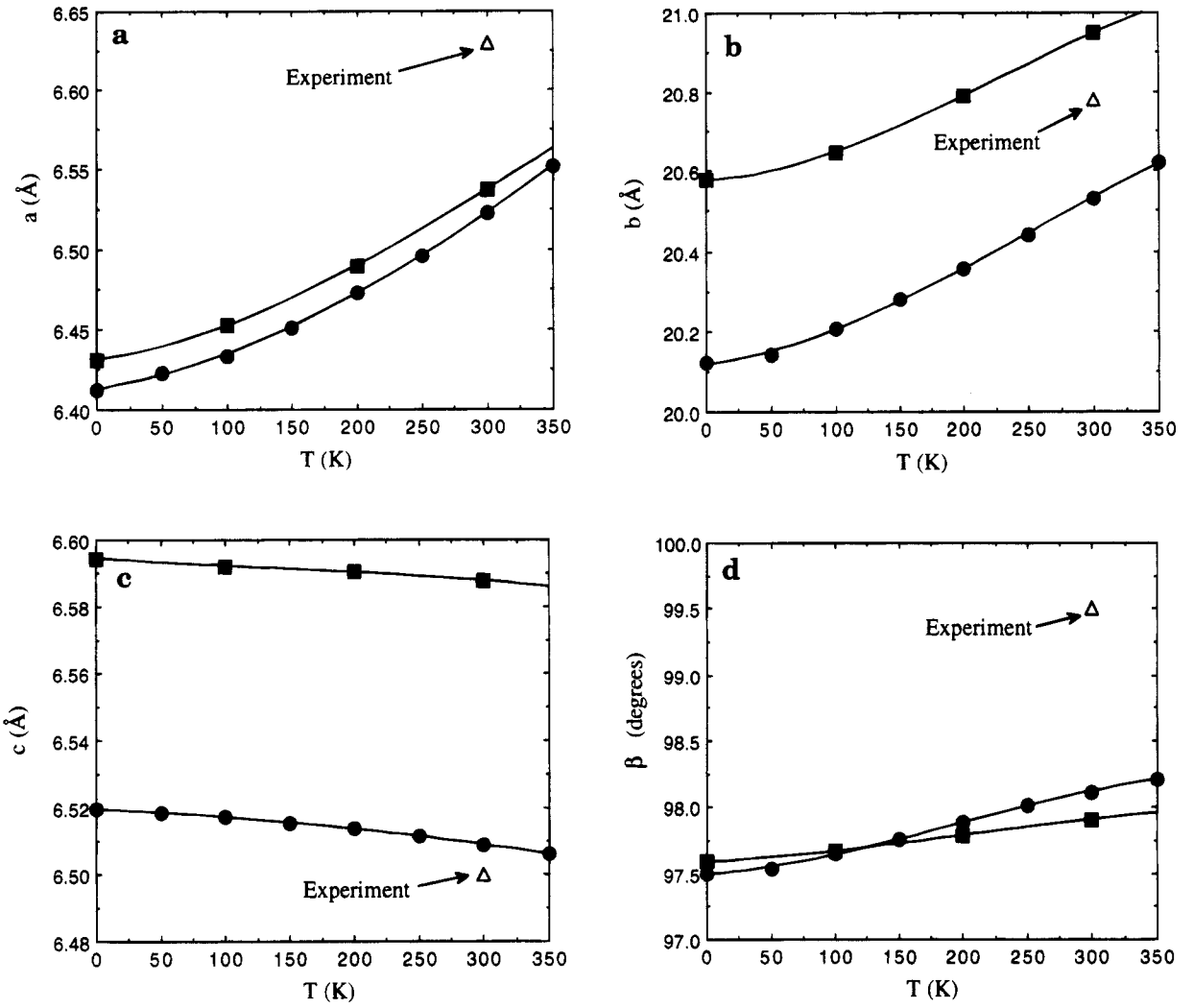


**Figure 2.** Lattice parameters of iPP as a function of temperature. The filled circles are the results with the SLKB* force field, the filled squares are the results with the KDG* force field, and the open triangles are the experimental results of Immerzi and Iannelli.[17]

**Table 2. Thermal Expansion at 300 K**

| | experiment | SLKB* | KDG* |
|---|---|---|---|
| $\alpha_1$ ($10^{-5}$ K$^{-1}$) | 6.2[a] | 8.2 | 7.3 |
| $\alpha_2$ ($10^{-5}$ K$^{-1}$) | 15[a] | 8.7 | 7.2 |
| $\alpha_3$ ($10^{-5}$ K$^{-1}$) | −1.0[b] | −0.84 | −0.48 |
| | −0.45[c] | | |

[a] Napolitano *et al.*[18] [b] Choy *et al.*[19] [c] Jawad *et al.*[20]

**Table 3. Isothermal Elastic Stiffness Constants[a]**

| | 0 K | 100 K | 200 K | 300 K |
|---|---|---|---|---|
| | | SLKB* | | |
| $C_{11}$ | 13.4 | 12.0 | 10.7 | 9.9 |
| $C_{22}$ | 12.6 | 12.3 | 11.1 | 10.8 |
| $C_{33}$ | 62.4 | 61.7 | 59.3 | 55.1 |
| $C_{44}$ | 3.5 | 3.7 | 3.9 | 4.0 |
| $C_{55}$ | 5.4 | 5.2 | 5.8 | 4.9 |
| $C_{66}$ | 5.2 | 4.5 | 4.3 | 1.7 |
| $C_{12}$ | 6.2 | 5.8 | 4.9 | 3.4 |
| $C_{13}$ | 10.1 | 9.4 | 8.3 | 7.1 |
| $C_{23}$ | 6.5 | 5.7 | 4.9 | 4.4 |
| | | KDG* | | |
| $C_{11}$ | 12.7 | 11.6 | 10.3 | 9.1 |
| $C_{22}$ | 11.5 | 11.7 | 9.3 | 8.6 |
| $C_{33}$ | 70.0 | 69.2 | 67.0 | 64.5 |
| $C_{44}$ | 4.1 | 3.6 | 4.4 | 4.3 |
| $C_{55}$ | 6.2 | 5.7 | 5.9 | 4.7 |
| $C_{66}$ | 5.8 | 4.3 | 4.1 | 3.5 |
| $C_{12}$ | 5.9 | 5.3 | 4.4 | 3.6 |
| $C_{13}$ | 8.8 | 8.4 | 7.5 | 7.2 |
| $C_{23}$ | 5.5 | 5.0 | 4.6 | 4.3 |

[a] The precision of these results is approximately ±1 GPa. The off-diagonal elements ($C_{x5}$ ($x$ = 1, 2, 3) and $C_{46}$ were all found to be less than 1 GPa, and the other $C_{xy}$ ($x \neq y$, $y$ = 4, 5, 6) are equal to zero by symmetry.

energy. The contribution of each of these effects to the temperature dependence of $C^T_{33}$ is shown in Table 5. The effects of the vibrational energy and entropy lead to less than half of the total temperature dependence of the axial stiffness modulus of iPP.

The temperature dependence of $C^T_{33}$ for iPP is also compared to that of other polymer crystals in Table 5, from which the relative importance of the factors affecting the temperature dependence of $C^T_{33}$ for the different polymers can be rationalized. First, the volume contribution is roughly proportional to the magnitude of the axial stiffness. The smaller effect (in absolute magnitude) of the volume increase in iPP as compared to the other polymer crystals (i.e., PE, PPTA and PBA) is due to the smaller magnitude of $C^T_{33}$ for iPP ($C^T_{33}$ is approximately 50 GPa for iPP, whereas $C^T_{33}$ is approximately 300 GPa for PE, PPTA, and PBA). Second, the magnitude of the decrease in the value of the second derivative of the potential energy can be related to differences between the crystalline $C^T_{33}$ and the corresponding single chain $C^T_{33}$. With thermal expansion the polymer chains move further apart and

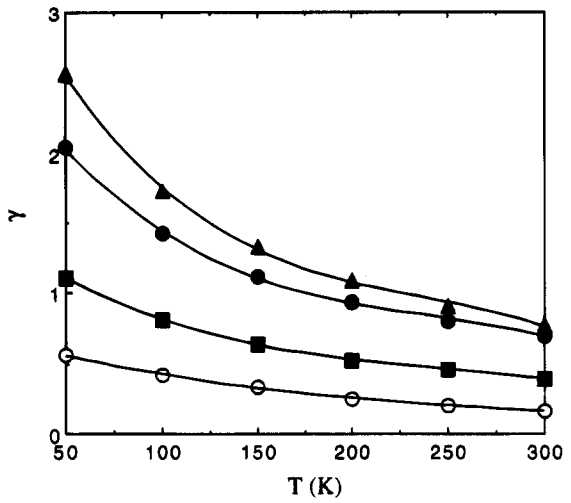


**Figure 3.** Gruneisen parameters for iPP as a function of temperature, calculated with the SLKB* force field. The filled circles are $\gamma_1$, the filled triangles are $\gamma_2$, the filled squares are $\gamma_3$, and the open circles are $2\gamma_5$. The Gruneisen parameters calculated with the KDG* force field are indistinguishable from those of the SLKB* force field.

**Table 4. Axial Thermal Expansion, in Units of $10^{-5}$ $K^{-1}$, at $T = 300$ K[a]**

| | $(C_v/V)\sum_{j=1}^{3}\gamma_j S^T_{3j}$ | $(C_v/V)[\gamma_1 S^T_{13} + \gamma_2 S^T_{23}]$ | $(C_v/V)\gamma_3 S^T_{33}$ |
|---|---|---|---|
| iPP (SLKB*) | −0.66 | −1.8 | +1.2 |
| iPP (KDG*) | −0.53 | −1.5 | +0.97 |
| PE (KDG) | −1.2 | −0.45 | −0.75 |

[a] The elastic coupling to the thermal shear stresses in iPP are neglected here.

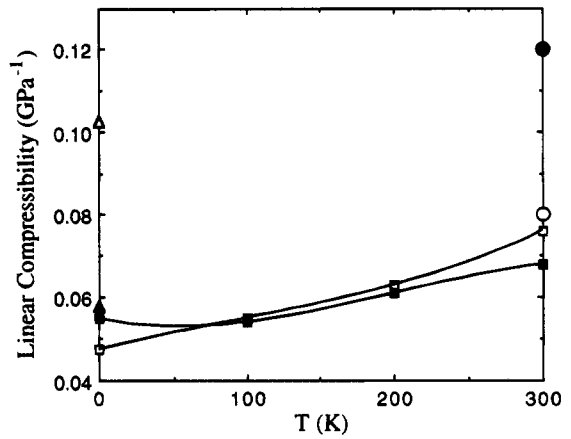


**Figure 4.** Linear compressibilities for iPP. Open symbols are for the $a$ axis; closed symbols are for the $b$ axis. Squares: SLKB* calculation. Triangles: calculation of Tashiro *et al.*[21] Circles: experimental results of Ito.[32] The KDG* results are similar to the SLKB* results and are omitted for clarity.

**Table 5. Contributions to the Decrease in $C^T_{33}$ with Temperature, in units of GPa/100 K**

| | total | 1/V | potential energy | vibrational free energy |
|---|---|---|---|---|
| iPP (SLKB*) | 3.5 | 1 | 1 | 1.5 |
| iPP (KDG*) | 2.5 | 1 | 0.5 | 1 |
| PE | 12 | 5 | 0 | 7 |
| PPTA | 7 | 2.5 | 2.5 | 2 |
| PBA | 8 | 2.5 | 2.5 | 3 |

the crystal becomes more like a collection of single chains, which are less constrained. The trends in the decrease in the value of the second derivative of the potential energy with temperature are consistent with results of earlier static–lattice calculations, which have shown a difference between the crystalline and single chain $C^T_{33}$ for iPP,[21] PPTA,[33,34] and PBA[34] but not for PE.[10] Third, the vibrational contribution to $C^T_{33}$, which is determined mainly by the value of the second derivative of the entropy, reflects the rigidity and the configuration of the polymer chain. The entropic contribution to $C^T_{33}$ is larger for PE than for iPP, even though both polymer chains are flexible, because the entropy changes more sharply with strain in the more taut all-trans configuration than in the looser helical configuration. Also, the entropic contribution is larger in PE than in PPTA and PBA because entropic effects are generally less important in the more rigid PPTA and PBA polymers.

*2. Other Stiffness Moduli.* The temperature dependence of the nonaxial stiffness moduli may be explained in similar terms. The transverse stiffness moduli, $C^T_{11}$ and $C^T_{22}$, decrease with temperature, the decrease for $C^T_{11}$ being larger than that for $C^T_{22}$. This decrease is due almost exclusively to the decrease in the value of the second derivative of the potential energy (mechanism 2), which occurs because the interchain interactions decrease as the polymer chains move further apart. The effect of the volume increase on the temperature dependence of $C^T_{11}$ and $C^T_{22}$ is relatively small.

As with the transverse elastic moduli, the off-diagonal elastic moduli would decrease with temperature based on potential energy effects alone because the interchain interactions decrease as the polymer chains move further apart. This is in fact observed for the $C^T_{12}$, $C^T_{13}$, and $C^T_{23}$ elastic moduli of iPP. Our calculations suggest that the temperature dependence of $C^T_{13}$ and $C^T_{23}$ of iPP differs from that found for PE and PBA, for which $C^T_{13}$ and $C^T_{23}$ were found to increase with temperature. This distinction is due to the greater entropic contributions to the elastic moduli (mechanism 3) in the latter cases.[2,3]

The shear moduli ($C^T_{ii}$, $i = 4, 5, 6$) are temperature-independent to within the accuracy of the current calculation. As with the transverse and off-diagonal stiffness moduli, a weak decrease in the shear elastic moduli would be expected based on potential energy effects alone.

## V. Conclusions

Finite temperature calculations of crystalline isotactic polypropylene were carried out. The results follow entirely from self-consistent lattice dynamics under the constraints of a molecular mechanics force field for the interatomic interactions and the quasi-harmonic approximation for the vibrational free energy, without any further assumptions.

The negative axial thermal expansion for iPP is due to elastic coupling to the thermal stresses transverse to the chain axis. The entropy decreases with chain contraction, which alone would lead to positive thermal expansion. Thus we predict that, if the transverse dimensions of the polymer crystal were not allowed to expand substantially upon heating, *positive* axial thermal expansion would occur. In contrast, our previous results showed that polyethylene undergoes negative axial thermal expansion due to an increase in entropy with chain contraction.[2] In this case the axial thermal expansion of polyethylene would remain negative even if the transverse dimensions of the crystal were constrained.

The decrease in the axial elastic modulus of iPP with temperature is due roughly in equal measure to the entropic contribution to the elastic modulus, and the

change in equilibrium volume and the shift of the system to a region of the potential energy surface with decreased curvature upon thermal expansion. The decrease in axial elastic modulus with temperature is significantly smaller in iPP than in PE. The entropic effect is smaller in iPP because of the looser helical chain configuration of iPP, and the effect of the increase in equilibrium volume is smaller because of the smaller elastic modulus of iPP. In crystalline polymers, it would appear that the entropic contribution to the axial elastic modulus is greatest for extended, dynamically flexible chains and is mitigated both by helicity of conformation and increased inherent rigidity.

**Acknowledgment.** The authors are grateful to Texaco for providing financial support for this work through the Texaco–Mangelsdorf Career Development Chair to G.C.R.

## References and Notes

(1) Tashiro, K. *Prog. Polym. Sci.* **1993**, *18*, 377.
(2) Lacks, D. J.; Rutledge, G. C. *J. Phys. Chem.* **1994**, *98*, 1222.
(3) Lacks, D. J.; Rutledge, G. C. *Macromolecules* **1994**, *27* (24), 7197.
(4) Lacks, D. J.; Rutledge, G. C. *Chem. Eng. Sci.* **1994**, *94* (17), 2881.
(5) Weiner, J. H. *Statistical Mechanics of Elasticity*; John Wiley & Sons: New York, 1983.
(6) Leibfried, G.; Ludwig, W. *Solid State Physics*; Seitz, F., Turnbull, D., Eds.; Academic Press: New York, 1961; Vol. 12, p 275.
(7) Born, M.; Huang, K. *Dynamical Theory of Crystal Lattices*; Oxford University Press: Oxford, 1954. Venkataraman, G.; Feldkamp, L. A.; Sahni, V. C. *Dynamics of Perfect Crystals*; MIT Press: Cambridge, MA, 1975.
(8) Lacks, D. J.; Rutledge, G. C. *J. Chem. Phys.* **1994**, *101* (11), 9961.
(9) Sorensen, R. A.; Liau, W. B.; Kesner, L.; Boyd, R. H. *Macromolecules* **1988**, *21*, 200.
(10) Karasawa, N.; Dasgupta, S.; Goddard, W. A. *J. Phys. Chem.* **1991**, *95*, 2260.
(11) Karasawa, N.; Goddard, W. A. *J. Phys. Chem.* **1989**, *93*, 7320.
(12) Hikosaka, M.; Seto, T. *Polym. J.* **1973**, *5*, 111.
(13) Corradini, P.; Petraccone, V.; Pirozzi, B. *Eur. Polym. J.* **1983**, *19*, 299.
(14) Ferro, D. R.; Bruckner, S.; Meille, S. V.; Ragazzi, M. *Macromolecules* **1992**, *25*, 5231.
(15) Natta, G.; Corradini, P. *Nuovo Cimento* **1960**, *15*, *Series X (supplement)*, 40.
(16) Mencik, Z. *J. Macromol. Sci., Phys.* **1972**, *B6*, 101.
(17) Immirzi, A.; Iannelli, P. *Macromolecules* **1990**, *21*, 768.
(18) Napolitano, R.; Pirozzi, B.; Varriale, V. *J. Polym. Sci.: Polym. Phys. Ed.* **1990**, *28*, 139.
(19) Choy, C. L.; Chen, F. C.; Ong, E. L. *Polymer* **1979**, *20*, 1192.
(20) Jawad, S. A.; Orchard, G. A. J.; Ward, I. M. *Polymer* **1986**, *27*, 1201.
(21) Tashiro, K.; Kobayashi, M.; Tadokoro, H. *Polym. J.* **1992**, *24*, 899.
(22) Sawatari, C.; Matsuo, M. *Macromolecules* **1989**, *22*, 2968. Sawatari, C.; Matsuo, M. *Macromolecules* **1986**, *19*, 2653.
(23) Peguy, A.; St. John Manley, R. *Polym. Commun.* **1984**, *25*, 39.
(24) Grubb, D. T. Elastic Properties of Crystalline Polymers. In *Materials Sciences and Technology*; Thomas, E. L., Ed.; VCH: New York, 1993; Vol. 12, p 301.
(25) Hsu, S. L.; Krimm, S.; Krause, S.; Yeh, G. S. Y. *J. Polym. Sci., Polym. Lett. Ed.* **1976**, *14*, 195.
(26) Chen, F. C.; Choy, C. L.; Young, K. *J. Polym. Sci., Polym. Phys. Ed.* **1980**, *18*, 2313. Chen, F. C.; Choy, C. L.; Wong, S. P.; Young, K. *J. Polym. Sci., Polym. Phys. Ed.* **1981**, *19*, 971.
(27) Baughman, R. H. *J. Chem. Phys.* **1973**, *58*, 2976.
(28) Choy, C. L.; Nakafuku, C. *J. Polym. Sci., Polym. Phys. Ed.* **1988**, *26*, 921.
(29) Kobayashi, Y.; Keller, A. Polymer **1970**, *11*, 114.
(30) Davis, G. T.; Eby, R. K.; Colson, J. P. *J. Appl. Phys.* **1970**, *41*, 4316.
(31) Choy, C. L. *Developments in Oriented Polymers*, Ward, I. M., Ed.; Applied Science Publishers: London, 1982; Vol. 1, p 121.
(32) Ito, T. *Polymer* **1982**, *23*, 1412.
(33) Rutledge, G. C.; Suter, U. W. *Polymer* **1991**, *32*, 2179.
(34) Yang, X.; Hsu, S. L. *Macromolecules* **1991**, *24*, 6680.

MA941120S